

Ionic fragmentation of the CO molecule by impact of 10-keV electrons: Kinetic-energy-release distributions

Raj Singh, Pragya Bhatt, Namita Yadav, and R. Shanker*

Atomic Physics Laboratory, Department of Physics, Banaras Hindu University, Varanasi 221005, India

(Received 3 December 2012; published 22 February 2013)

The ionic fragmentation of a multiply charged CO molecule is studied under impact of 10-keV electrons using recoil-ion momentum spectroscopy. The kinetic-energy-release distributions for the various fragmentation channels arising from the dissociation of CO^{q+} ($q = 2-4$) are measured and discussed in light of theoretical calculations available in the literature. It is observed that the present kinetic-energy-release values are much smaller than those predicted by the Coulomb explosion model. The kinetic-energy-release distribution for the $\text{C}^+ + \text{O}^+$ channel is suggested to arise from the tunneling process. It is seen that the peak of kinetic-energy-release distribution is larger for that dissociation channel that arises from the same molecular ion which has higher charge on the oxygen atom. Further, the relative ionic fractions for seven ion species originating from ionization and subsequent dissociation of the CO molecule are obtained and compared with the existing data reported at low energy of the electron impact. The precursor-specific relative partial ionization cross sections are also obtained and shown to be about 66.4% from single ionization, 29.9% from double ionization, 3.3% from triple ionization, and about 0.4% from quadruple ionization of the precursor CO molecule contributing to the total fragment ion yield.

DOI: [10.1103/PhysRevA.87.022709](https://doi.org/10.1103/PhysRevA.87.022709)

PACS number(s): 34.80.Gs, 34.80.Ht

I. INTRODUCTION

The fragmentation dynamics of a multiply charged molecule induced by charged particles and photons is a very active area of research in recent times [1–6]. It has wide applications in the field of science and technology because it helps to explore the details of collision induced processes in the field of astrophysics, atmospheric physics, plasma physics, and radiation damage of biological systems [7–9]. Carbon monoxide (CO) is the second most abundant molecule in space after molecular hydrogen [10]. It is also found in the atmosphere of some comets [11]. The CO^+ ion has been observed in the interstellar space [12]. Cosmic rays (fast-moving protons and electrons) present in the interstellar space induce the fragmentation of molecules present in it and the fragment ions produced from such collisions play a very important role in the formation of complex molecules [13]. Hence the study of fragmentation dynamics of a CO molecule induced by the energetic particles sheds light on the chemical and the physical processes occurring in the interstellar space. The partial ionization cross sections (PICSSs) ([14–17] and references therein) and the fragmentation dynamics of the CO molecule have been studied by many workers in the past [18–27]. Most of the studies were devoted to the electronic states of singly charged molecular ion and/or of the fragmentation channel $\text{C}^+ + \text{O}^+$ arising either from the dissociation of a CO^{2+} ion or from the autoionization of a highly excited CO^+ ion with the impact of low-energy electrons and photons [3,4,18–20]. Few studies have been devoted to examining the multiply charged molecular ions of CO using different experimental techniques by the impact of ions and the intense laser fields [5,21–26]. However, the study of fragmentation of a multiply charged CO molecule produced from the impact of energetic electrons is scarce. In such a

case, the multiple ionization of the molecule is produced by the direct energy transfer from energetic electrons (direct ionization) and by the contribution from the indirect processes (Auger-like autoionization). For the case of a CO molecule, the threshold energies for the formation of single, double, triple, and quadruple ionization are 14.0 eV, 41.0 eV, 84.0 eV, and 150.0 eV, respectively [15]. The production of these multiple ionization states depends on the impact energy of the electrons. The low-energy electrons transfer more energy to the target molecule than the energetic electrons because the interaction time for low-energy electrons with molecules is larger compared to the energetic electrons. The electrons have only the kinetic energy, while the swift highly charged ions (MeV) and strong laser fields have also extremely high potential-energy fields [28]. Due to this, the highly charged ions capture the electrons from the target molecule and produce highly charged molecular ions. Similarly, when a molecule is exposed to an extremely high potential-energy field of lasers, many electrons can be stripped out from the molecule. The difference between the strong laser field and the swift highly charged ions occurs due to the interaction time. The strong laser field has the interaction time of the order of molecular vibration ($\sim 10^{-14}$ s) and rotation times ($\sim 10^{-12}$ s), while the interaction time for swift ions is of the order of subfemtosecond. Further, the typical interaction time for the collision induced by energetic electron is of the order of subfemtosecond; therefore, the molecular excitation is a Franck-Condon process and kinetic-energy release depends on the internuclear distance at the time of excitation [6]. The electron-impact-induced fragmentation of the molecule can provide information about different electronic states of the multiply charged molecular ion. A large number of theoretical studies have been made on the potential-energy surfaces of CO^+ and CO^{2+} ions [19,20,27,29–31], while only a few studies are available for triply and higher charged molecular ions [6,32]. The advent of position sensitive detectors coupled with a time of flight (TOF) spectrometer enables us to detect

*shankerorama@gmail.com

correlated fragment ions with their respective positions and time of flight information which, in turn, provide valuable information on the fragmentation dynamics of the precursor molecule. Such experiments make it possible to obtain improved information on the kinetic-energy-release distributions (KERDs), branching ratios of various fragmentation channels, and on the stability of molecular ions. These inputs play an important role in evaluating the validity of the theoretical calculations of the molecular potential-energy surfaces (PESs) [27,32].

In the present paper, we report on the experimental results of the fragmentation processes of the CO molecule induced by 10-keV electrons using recoil-ion momentum spectroscopy. The KERDs for various dissociation channels arising from the dissociation of CO^{q+} ($q = 2-4$) are determined and discussed in light of theoretical calculations available on the PESs for these molecular ions. The peak values of KERDs are also compared with the KER values predicted by the Coulomb explosion (CE) model and those reported by other workers. Further, the relative ionic fractions (RIFs) for different ion species originating from the ionization and subsequent dissociation of the CO molecule are measured. The precursor-specific relative partial ionization cross sections (PICSSs) are also determined for the five fragment ions. In addition, we have estimated the contributions of single, double, triple, and quadruple ionization of CO to the total fragment ion yield.

II. EXPERIMENTAL SETUP AND DATA ANALYSIS

The experimental setup and data analysis procedures are described in detail in our previous publications [33,34]. Briefly, a monoenergetic beam of 10-keV electrons extracted from an electron gun is made to collide with CO molecules (99.99%) effusing from a hypodermic needle (length = 1.2 cm; diameter = 0.01 cm). A single stage linear time-of-flight (TOF) mass spectrometer coupled with a position sensitive detector was used to detect and analyze the mass-to-charge ratios of the fragment ions. The electron beam, the CO gas jet, and the axis of the TOF spectrometer were aligned orthogonal to each other. The electrons and positive ions produced from a single collision event were extracted from the collision zone by applying a homogeneous electric field of 174 V/cm; electrons were detected by a channeltron mounted in the opposite direction to that of the ion detector and were used as the timing reference for ion arrivals to a dual microchannel plate (MCP). The data was stored in an event by event mode and analyzed off-line by using the Cobold PC software. The ion-detection efficiency (D) of our setup is estimated to be $\sim 24\%$ [34]. We have taken the same detection efficiency for all ions observed in the present experiment.

The collision events in which one fragment ion and the correlated electron are measured in coincidence give rise to a time-of-flight (TOF) (singles) spectrum, while events in which two fragment ions and the correlated electrons are detected in coincidence yield an ion-ion coincidence map (doubles spectrum). The TOF spectrum and the ion-ion coincidence map are shown in Figs. 1 and 2, respectively. We subtracted the background from the TOF spectrum following the same procedure as given in [35]. To subtract the random coincidences from the ion-ion coincidence map, we took into

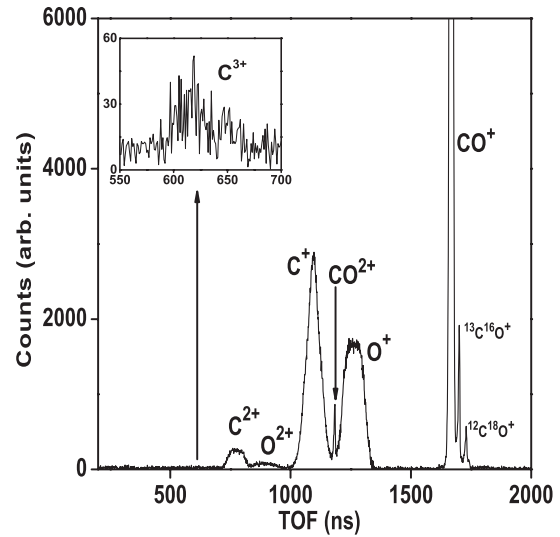


FIG. 1. TOF spectrum (background subtracted) of the produced ions following direct and dissociative ionization of a CO molecule by impact of 10-keV electrons. The C^{3+} ion peak is shown in the inset.

account only those counts which follow the law of momentum conservation. In order to obtain the RIF, the background subtracted ion counts $N(X^+)$ are estimated from the TOF spectrum, where $X^+ = \text{CO}^+, \text{CO}^{2+}, \text{C}^+, \text{O}^+, \text{C}^{2+}, \text{O}^{2+}$, and C^{3+} ; when these ion counts are divided by the sum of all counts of ions, the RIF for the X^+ ion is obtained. Further, to obtain the precursor specific PICSSs, we took the random coincidence corrected data which are also corrected for detection efficiency D and D^2 for the TOF spectrum and the ion-ion coincidence map, respectively. To get the events arising only from singly ionized molecules, the count considered from the TOF spectrum is corrected by subtracting the contribution of events arising from the doubly, triply, and quadruply ionized CO molecule with consideration of the detection efficiency as

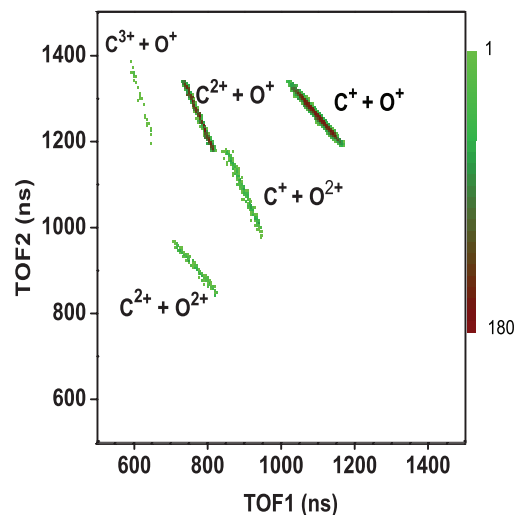


FIG. 2. (Color online) Ion-pairs spectrum resulting from dissociative ionization of CO^{q+} ($q = 2-4$) produced in 10-keV electron collisions with CO molecule.

given below [34]:

$$N_{\text{corr}}(X^+) = \frac{N(X^+)}{D} - \sum_{Y^{n+}} \frac{N(X^+ + Y^{n+})}{D^2}, \quad n + 1 \leq 4,$$

$$N_{\text{corr}}(\text{CO}^+) = \frac{N(\text{CO}^+)}{D}.$$

The relative precursor specific PICSs (σ_1) for ion X^+ are obtained when the corrected counts $N_{\text{corr}}(X^+)$ are divided by $N_{\text{corr}}(\text{CO}^+)$; similarly, σ_2 , σ_3 , and σ_4 are estimated by considering the events arising only from double, triple, and quadruple ionization of CO, respectively. The RIFs, the precursor specific PICSs, and the involved errors are estimated by using the analysis procedures given in [34,36]. The overall uncertainties in the presented data for each ion single are 2.5%, <4%, 4%, 10%, 6%, 8%, and 15%, for CO^+ , C^+ , O^+ , CO^{2+} , C^{2+} , O^{2+} , and C^{3+} , respectively. For all observed five channels as shown in Fig. 2, wherein the complete Coulomb fragmentation processes occur, we consider only those counts which obey the law of momentum conservation. The errors for RIFs and precursor-specific relative PICSs are calculated using the above given uncertainties for each ion single. The momentum vectors of fragment ions detected in coincidence are calculated from their respective TOFs (t) and positions (x, y) on the MCP [33]. The kinetic energy of individual fragment ions is determined from their momentum vectors and the total KER is obtained from the sum of the kinetic energies of individual fragments involved in that particular dissociation channel. The slope and size of the islands in the ion-ion coincidence map were used to obtain information regarding the nature of dissociation mechanism [37,38].

III. RESULTS AND DISCUSSION

The background subtracted TOF spectrum of ions produced from direct and/or indirect ionization of the CO molecule under impact of 10-keV electrons is shown in Fig. 1. We observe sharp peaks of CO^+ and CO^{2+} ions having thermal energies. These ionic peaks arise from direct ionization of the CO molecule. Additionally, five ion fragments (O^+ , C^+ , O^{2+} , C^{2+} , and C^{3+}) are also formed which arise from the dissociative ionization of the multiply charged CO^{q+} ($q \leq 4$) ions. The CO^+ peak is the most intense peak in the TOF mass spectrum. The two peaks adjacent to the CO^+ peak on the right side are attributed to $^{13}\text{C}^{16}\text{O}$ and $^{12}\text{C}^{18}\text{O}$ isotopes whose natural abundances are found to be 1.1% and 0.25%, respectively. The CO^{2+} is a quasistable molecular ion which is found to have a lifetime of 1.19 μs in our experiment. Many workers have reported its mean lifetime ranging from 1 to 30 μs in TOF measurements ([16] and references therein). However, the long-lived (>3.8 s) CO^{2+} ion has been observed in the ion storage rings; it has also been shown theoretically that the lifetime of this ion depends on the involved metastable electronic states [39]. From the ion-ion coincidence map, five dissociation channels ($\text{C}^+ + \text{O}^+$, $\text{C}^{2+} + \text{O}^+$, $\text{O}^{2+} + \text{C}^+$, $\text{C}^{2+} + \text{O}^{2+}$, and $\text{C}^{3+} + \text{O}^+$) originating from the complete Coulomb dissociation of CO^{q+} ($q = 2-4$) are observed (see Fig. 2). It is found that the islands of these channels are narrow and their observed slopes are according to the slopes calculated using the formulation given in [37,38] (see Table I). It is due to the fact that the

TABLE I. Relative intensities and theoretical and experimental slopes of islands in an ion-ion coincidence map for different dissociation channels produced from dissociation of CO^{q+} ($q = 2-4$) in 10-keV electron impact with CO. The KER values calculated from the CE model (KER_{CEM}) is also included in the table.

Channels	KER_{CEM} (eV)	Relative intensity (%)	Theoretical slope (deg)	Observed slope (deg)
$\text{C}^+ + \text{O}^+$	12.8	87.9	-45.0	-45.0 ± 1.0
$\text{C}^{2+} + \text{O}^+$	25.5	8.7	-63.4	-63.3 ± 1.0
$\text{C}^+ + \text{O}^{2+}$	25.5	2.2	-63.4	-63.3 ± 1.0
$\text{C}^{2+} + \text{O}^{2+}$	51.0	1.0	-45.0	-45.0 ± 1.0
$\text{C}^{3+} + \text{O}^+$	38.3	0.2	-71.6	-71.0 ± 1.0

fragment ions fly back to back to obey the momentum conservation law. The KER values for these channels are calculated by using the CE model at equilibrium internuclear distance of 1.128 Å of CO molecules [27]. The calculated KER values and the relative intensity for these channels are also given in Table I. The branching ratios, the precursor specific PICSs, and the KERDs are discussed in detail in the following sections.

A. RIFs and precursor-specific relative PICSs

The RIFs for various ion species originating from the collisions of a CO molecule with 10-keV electrons are given in Table II. No other data at this impact energy is available in the literature to compare directly with our results. Under the assumption that the RIF for the ion species formed from a collision event is invariant under impact energies above certain values, we have compared our data with those available in the literature for the low-energy electron impact (shown in Table II). In the case of a CO molecule, it has been found that, after 500 eV, the RIFs for the ions arising from singly, doubly, triply, and quadruply ionized molecular ions are almost constant [15]. The RIF of CO^+ shows a good agreement with the data of Tian and Vidal [14] and Mangan *et al.* [16] within 4%. But, a deviation of about 13% is observed with the data of Orient and Srivastava [17]. Our results for C^+ and O^+ fragment ions agree with the data of Tian and Vidal [14] and Mangan *et al.* [16], while it is seen to be about 14% higher for C^+ and about three times larger for O^+ than that of Orient and Srivastava

TABLE II. Comparison of the RIFs for formation of the single ions produced in 10-keV electron impact with a CO molecule with the results reported at low electron-impact energies.

Ion species	RIFs (%)			
	Present 10 keV	1 keV ^a	0.6 keV ^b	0.51 keV ^c
CO^+	76.4 ± 1.9	79.2	78.0	86.6
C^+	11.5 ± 0.4	11.4	11.5	9.9
O^+	9.8 ± 0.4	9.5	9.4	3.5
CO^{2+}	0.42 ± 0.04	0.34	0.30	
C^{2+}	1.20 ± 0.07		0.64	
O^{2+}	0.52 ± 0.04		0.16	
C^{3+}	0.10 ± 0.02			

^aReference [16].

^bReference [14].

^cReference [17].

[17]. This mismatch possibly suggests the loss of energetic O^+ ions in the experiments of later authors. It is found that our RIF for a CO^{2+} molecular ion is 29% and 19% higher than those of Tian and Vidal [14] and Mangan *et al.* [16], respectively; however, Orient and Srivastava [17] did not observe this molecular ion in their experiment. This may be due to the reason that the impact energy used by Orient and Srivastava [17] is below the $O(1s)$ ionization potential (542.5 eV) [40]. The RIF for C^{2+} and O^{2+} ion fragments is about two and three times larger than the respective RIFs of Tian and Vidal [14], while Mangan *et al.* [16] and Orient and Srivastava [17] did not observe these fragment ions in their experiments. We have also observed C^{3+} fragment ion. It is obvious from the above comparisons that the RIFs for CO^{2+} , C^{2+} , O^{2+} , and C^{3+} ions at our electron-impact energy are generally higher than those at lower electron-impact energies. The RIFs for CO^+ , C^+ , and O^+ show reasonably good agreement with those at low-energy electron impact because they possibly arise from the dipole allowed transitions, whereas the mismatch in the RIF values for CO^{2+} , C^{2+} , O^{2+} , and C^{3+} may arise due to the involvement of the dipole nonallowed transitions. In our earlier experiments, we have also observed the large RIF for doubly charged ions [34,36]. It has been shown [41] that at higher impact energies the multiple ionization is governed mainly by Auger-like-autoionization processes followed by creation of a vacancy in the inner-shell molecular orbital. Therefore, the dominance of Auger-like autoionization may be responsible for the enhanced production of doubly and triply ionized ion fragments.

The precursor-specific relative PICSSs σ_n ($n = 1-4$) for the fragment ions formed from the collisions of a CO molecule with 10-keV electrons are given in Table III. The precursor-specific relative PICSSs σ_1 , σ_2 , σ_3 and σ_4 show the contributions from singly, doubly, triply, and quadruply ionized CO molecules to a particular ion yield, respectively. The PICSS (σ_n) is obtained from the sum of the precursor-specific relative PICSSs of individual ion fragments from these ionization states and they are shown in the last column of Table III. We also find that about 66.4% of single ionization, 29.9% of double ionization, 3.3% of triple ionization, and about 0.4% of quadruple ionization of the precursor CO molecule contribute to the total fragment ion yield. This leads to a result that the multiple ionization (33.6%) of the CO significantly contributes to the total fragment ion yield.

B. Fragmentation of CO^{2+}

A typical ion-ion coincidence spectrum resulting from the collision of 10-keV electrons with CO is displayed in Fig. 2;

TABLE III. Precursor-specific partial ionization cross sections, σ_n ($n = 1-4$) ($\times 10^{-2}$), for fragment ions produced in collisions of 10-keV electrons with CO expressed relative to the cross section for formation of CO^+ ; the suffix n denotes the ionization state of CO after the removal of n number of electrons.

Ion species	σ_1	σ_2	σ_3	σ_4	PICSS = $\Sigma\sigma_n$
C^+	11.2 ± 0.6	3.8 ± 0.2	0.1 ± 0.01		15.10
O^+	8.9 ± 0.4	3.50 ± 0.03	0.37 ± 0.02	0.010 ± 0.002	12.80
C^{2+}		1.16 ± 0.06	0.34 ± 0.02	0.042 ± 0.005	1.54
O^{2+}		0.58 ± 0.04	0.055 ± 0.003	0.042 ± 0.005	0.68
C^{3+}			0.12 ± 0.01	0.010 ± 0.002	0.13

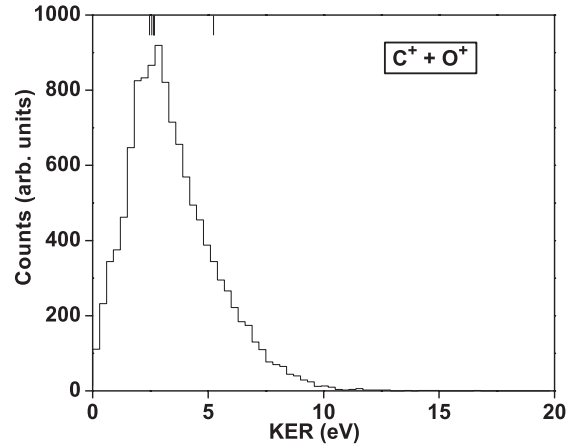


FIG. 3. KER distribution for the channel: $C^+ + O^+$ observed in the dissociation of CO^{2+} in 10-keV electron impact with CO. Theoretical values derived from the relevant states involved in this dissociation channel are shown in Table IV. These values are marked by the vertical lines at the top of the graph.

the resulting fragmentation channels are labeled in the figure. The $C^+ + O^+$ channel arising from the dissociation of CO^{2+} is the most dominant dissociation channel among all observed channels (see Table I). The KERD for this channel is shown in Fig. 3. The peak of the KERD is found to be at 2.8 ± 0.3 eV which is much smaller than the KER value predicted by the CE model (see Table I). To account for the KER distribution for this channel, we consider only three low-lying states of CO^{2+} ion from [20]; the molecular states, their associated KER values, vertical energy for different CO^{2+} states, and the dissociation limits for these states are given in Table IV. The values of $C^+(^2P) + O^+(^2D)$ and $C^+(^2P) + O^+(^4S)$ dissociation limits are 39.30 eV and 35.98 eV, respectively, relative to the ground state of a CO molecule at the equilibrium internuclear distance [30]. Table IV indicates that the $^1\Sigma^+$ and $^1\Pi$ states significantly contribute to the KERD, while the contribution of the $^3\Pi$ state is probably smaller. The metastable states $^1\Sigma^+$ and $^1\Pi$ most probably dissociate into $C^+(^2P) + O^+(^2D)$ by tunneling through the potential barrier because their coupling with the $^3\Sigma^-$ repulsive state yields a KER value above 5.0 eV [20,29]. However, the $^3\Pi$ state predissociates via the $^3\Sigma^-$ repulsive state into $C^+(^2P) + O^+(^4S)$ [20]. The KERD for this channel has been reported by many workers with the impact of ions, low-energy electrons, intense laser fields, and photons (see Table V). Most of them have reported the peak value of KERD above 5.0 eV. However, from the

TABLE IV. Possible molecular states of CO^{2+} dissociating into $\text{C}^+ + \text{O}^+$ along with the theoretically calculated values of KER.

Molecular states	Vibrational levels	KER (eV)	Vertical energy (eV) ^a	Dissociation limit ^c	Dissociation limit value (eV) ^c
$^3\Pi$	0	5.31	41.29 ^b	$\text{C}^+(^2P) + \text{O}^+(^4S)$	35.98
$^1\Sigma^+$	0	2.39	41.69	$\text{C}^+(^2P) + \text{O}^+(^2D)$	39.30
	1	2.64	41.94		
$^1\Pi$	0	2.52	41.82	$\text{C}^+(^2P) + \text{O}^+(^2D)$	39.30
	1	2.70	42.00		

^aReference [20].

^bReference [31].

^cReference [30].

ion impact, Ben-Itzhak *et al.* [24] and Tarisien *et al.* [27] have obtained the KER component below 5 eV; they have concluded that this KER component arises due to the dissociation of a metastable CO^{2+} molecular ion via the tunneling process. It is noted that the KERD has a long tail which may arise due to the participating higher states of the CO^{2+} ion. From the above discussions, it may be stated that the low value of KER corresponds to the involvement of those dicationic states that are metastable. In view of the variation of KER values obtained by different workers with their excitation sources and energies, some complex dynamics is envisaged between decay via tunneling through the potential barrier on one hand and the interaction time on the other hand.

C. Fragmentation of CO^{3+}

From Fig. 2, we observe two fragmentation channels: $\text{C}^{2+} + \text{O}^+$ and $\text{C}^+ + \text{O}^{2+}$ which arise from the fragmentation of the CO^{3+} molecular ion. It is seen that the relative intensity for the $\text{C}^{2+} + \text{O}^+$ channel is relatively larger than that for the $\text{C}^+ + \text{O}^{2+}$ channel (see also Table I). Similar results have been noted by other workers [6,19,24]. The difference in the relative intensity between the two channels is attributed to the nature of dissociation dynamics because the lower dissociation limit for $\text{C}^+ + \text{O}^{2+}$ lies about 11.0 eV above the lowest dissociation limit for the $\text{C}^{2+} + \text{O}^+$ channel [42]. The KERDs for both channels are shown in Fig. 4. The peak values of KERD

for the channels $\text{C}^{2+} + \text{O}^+$ and $\text{C}^+ + \text{O}^{2+}$ are found to be 11.5 ± 0.4 eV and 17.0 ± 0.4 eV, respectively. These KER values are smaller than the KER values calculated from the CE model. Different electronic states of the CO^{3+} molecular ion, the calculated KER values, and the dissociation limits for both channels are listed in Table VI (taken from [32,43]). For both channels, the theoretically calculated KER values show a reasonably good agreement with our observed KER values. Some workers have reported the KER values for these channels under the impact of ions (see Table V). It is found that their KER values are larger than the KER values obtained in the present experiment. Furthermore, Wei *et al.* [5] have observed the KER value for both channels from the interaction of intense laser fields with the CO molecule, which is shown to be about 12.0 eV for both channels. It is seen that our KER value for channel $\text{C}^{2+} + \text{O}^+$ finds a good agreement with that of Wei *et al.* [5], while our KER value for $\text{C}^+ + \text{O}^{2+}$ channel is larger than that of Wei *et al.* [5]. It may be noted here that the larger KER values observed in the experiments with the ion impacts are possibly due to the excitation of higher electronic states of the CO^{3+} ion in these experiments.

D. Fragmentation of CO^{4+}

The fragmentation of the CO^{4+} molecular ion gives rise to two dissociation channels $\text{C}^{2+} + \text{O}^{2+}$ and $\text{C}^{3+} + \text{O}^+$ (see Fig. 2). It is clear from the figure as well as from Table I

TABLE V. Comparison of kinetic-energy release in different dissociation channels obtained by impact of 10-keV electrons on CO with the earlier reported experimental results.

Dissociation channel	KER (eV)							
	Electron impact			Ion impact			Photon impact	
	Present	200 eV ^a	11.4 MeV/u O^{7+} ions ^b	1.2 MeV/u Ar^{8+} ions ^c	1.0 MeV/u F^{4+} ions ^d	Intense laser field 820 nm (10^{14} W/cm ²) ^e	44 eV ^f	306.4 eV ^g
$\text{C}^+ + \text{O}^+$	2.8 ± 0.3	7.8	6.5	6.2	12.0	6.74	6.0	9.5
$\text{C}^{2+} + \text{O}^+$	11.5 ± 0.4			17.5	27.0	11.87		
$\text{C}^+ + \text{O}^{2+}$	17.0 ± 0.4			28.0	39.0	12.17		
$\text{C}^{2+} + \text{O}^{2+}$	23.5 ± 0.5			48.0	49.0	22.11		

^aReference [20].

^bReference [27].

^cReference [6].

^dReference [24].

^eReference [5].

^fReference [19].

^gReference [3].

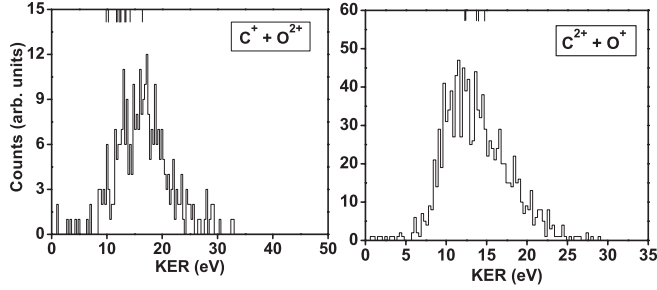


FIG. 4. KER distributions for the channels: $C^+ + O^{2+}$ and $C^{2+} + O^+$ observed in the dissociation of CO^{3+} in 10-keV electron impact with CO. Theoretical values derived from the relevant states involved in this dissociation channel are shown in Table VI. These values are marked by the vertical lines at the top of the graph.

that the symmetric channel $C^{2+} + O^{2+}$ occurs more frequently than the asymmetric channel. The KERD for the channel $C^{2+} + O^{2+}$ is shown in Fig. 5. The peak value of KER is observed at 23.5 ± 0.4 eV, which is also much smaller than the KER value calculated by using the CE model. The KERD for the channel $C^{3+} + O^+$ is not shown due to its low statistics; however, it is found that it has a distribution between 7 eV and 35 eV. The molecular states of the CO^{4+} ion, their associated KER, and the dissociation limits for different molecular states are listed in Table VII (the value of KER and the dissociation limit are calculated using the values taken from [5,6,43]). It is obvious from Table VII that the calculated KER values explain the KERD; the high-energy side of KERD may be arising either from higher states of the CO^{4+} molecular ion or from the lower dissociation limits. It is observed that our KER value is much smaller than those of the ion impacts in general, whereas it shows a reasonable agreement with the KER value reported from the interaction of intense laser field (see Table V). In passing, it may be mentioned here that there are no experimental data

TABLE VI. Possible molecular states of CO^{3+} dissociating into $C^+ + O^{2+}$ and $C^{2+} + O^+$ with theoretically calculated values of KER taken from [32,43].

Molecular states	KER (eV)	Dissociation limit	Dissociation limit value (eV)
$^2\Pi$	12.27	$C^{2+}(^3P) + O^+(^2D)$	68.67
	8.91	$C^+(^2P) + O^{2+}(^1S)$	72.04
	11.83	$C^+(^2P) + O^{2+}(^3P)$	69.12
$^4\Pi$	14.07	$C^{2+}(^3P) + O^+(^2D)$	68.67
	13.62	$C^+(^2P) + O^{2+}(^3P)$	69.12
$^6\Pi$	16.47	$C^+(^4P) + O^{2+}(^3P)$	71.32
	13.74	$C^{2+}(^3P) + O^+(^2D)$	68.67
$^2\Sigma^+$	10.38	$C^+(^2P) + O^{2+}(^1S)$	72.04
	13.30	$C^+(^2P) + O^{2+}(^3P)$	69.12
	13.04	$C^{2+}(^3P) + O^+(^2D)$	68.67
$^2\Sigma^-$	12.59	$C^+(^2P) + O^{2+}(^3P)$	69.12
	12.41	$C^{2+}(^3P) + O^+(^2D)$	68.67
$^4\Sigma^-$	11.97	$C^+(^2P) + O^{2+}(^3P)$	69.12
	14.73	$C^{2+}(^3P) + O^+(^2D)$	68.67
$^2\Delta$	14.28	$C^+(^2P) + O^{2+}(^3P)$	69.12
	12.08	$C^+(^4P) + O^{2+}(^3P)$	71.32

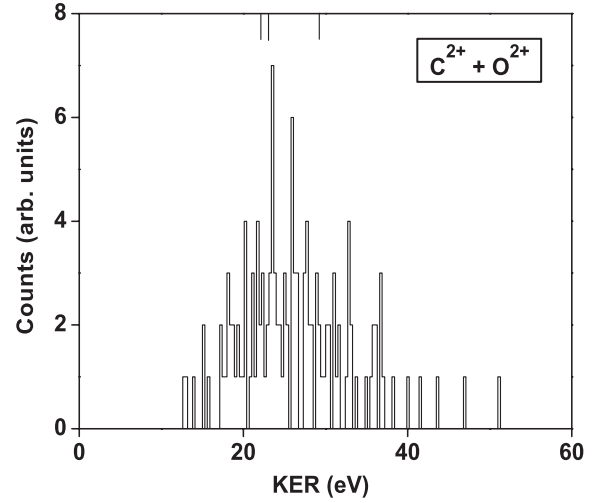


FIG. 5. KER distribution for the symmetric channel: $C^{2+} + O^{2+}$ observed in the dissociation of CO^{4+} in 10-keV electron impact with CO. Theoretical values derived from the relevant states involved in this dissociation channel are shown in Table VII. These values are marked by the vertical lines at the top of the graph.

available in the literature for dissociative ionization of CO^{4+} ions under impact of electrons of considered energy with which to compare. Hence further studies are required to gain detailed knowledge of dissociative ionization of this precursor ion.

IV. CONCLUSIONS

We have studied the formation and subsequent dissociation of a multiply charged CO molecule under the impact of 10-keV electrons using a position sensitive detector with multihit ability coupled with a time-of-flight spectrometer. Five dissociation channels arising from the dissociation of CO^{q+} ($q = 2-4$) ions are observed and identified. It is found that the channel $C^{2+} + O^+$ occurred more frequently than the channel $C^+ + O^{2+}$ produced from the dissociation of the CO^{3+} molecular ion. The dominance of the symmetric channel over the asymmetric channel is clearly observed for the dissociation of a CO^{4+} molecular ion. The KERDs for different channels produced from the dissociation of CO^{q+} ($q = 2-4$) are obtained and compared with the CE model and with those reported by other workers. For all channels, the observed KERs are found to be smaller than the KER values predicted by the CE model. The KERD for the $C^+ + O^+$ dissociation channel mainly arises due to the tunneling process. Furthermore, we obtain the RIFs for seven ion species originated from the dissociation of the CO

TABLE VII. Possible molecular states of CO^{4+} dissociating into $C^{2+} + O^{2+}$ and theoretically calculated values of KER from [5,6,43].

Molecular states	KER (eV)	Dissociation limit	Dissociation limit value (eV)
$^3\Pi$	22.98	$C^{2+}(^1D) + O^{2+}(^3P)$	112.45
$^3\Delta$	21.99	$C^{2+}(^1D) + O^{2+}(^1S)$	117.80
$^1\Delta$	29.27	$C^{2+}(^1D) + O^{2+}(^1D)$	114.96

molecule under the impact of 10-keV electrons. The present results on the RIF for C^{2+} and O^{2+} ions are respectively almost two and three times larger than those of other workers for low-energy electron impact. The precursor-specific relative PICSS are also obtained and it is found that the multiple ionization (33.6%) of the CO molecule contributes significantly next to the dominating single ionization to the total fragment ion yield.

ACKNOWLEDGMENTS

The work was supported by the Department of Science and Technology (DST), New Delhi under the research project SR/S2/LOP-09/2006. R.S., N.Y., and P.B. thankfully acknowledge partial support by Council of Scientific and Industrial research, New Delhi (CSIR) and Board of research in Fusion Science & Technology, Ahmedabad (BRFST) during the progress of this work.

-
- [1] D. Mathur, *Phys. Rep.* **391**, 1 (2004).
[2] S. D. Price, *Phys. Chem. Chem. Phys.* **5**, 1717 (2003).
[3] Th. Weber *et al.*, *J. Phys. B* **34**, 3669 (2001).
[4] T. Osipov *et al.*, *Phys. Rev. A* **81**, 011402(R) (2010).
[5] G. Wei, Z. Jing-Yi, W. Bing-Xing, W. Yan-Qiu, and W. Li, *Chin. Phys. Lett.* **26**, 013201 (2009).
[6] J. Rajput and C. P. Safvan, *Phys. Rev. A* **75**, 062709 (2007).
[7] A. Qayyum, W. Schustereder, C. Mair, W. Hess, P. Scheier, and T. D. Mark, *Phys. Scr.*, **T 103**, 29 (2003).
[8] B. Boudaiffa, P. Cloutier, D. Hunting, M. A. Huels, and L. Sanche, *Science* **287**, 1658 (2000).
[9] S. D. Price, *Int. J. Mass Spectro.* **260**, 1 (2007).
[10] J. H. D. Eland, M. Hochlaf, G. C. King, P. S. Kreyenin, R. J. LeRoy, I. R. McNab, and J.-M. Robbe, *J. Phys. B* **37**, 3197 (2004).
[11] H. A. Weaver, P. D. Feldman, M. F. A'Hearn, N. Dello Russo, and S. A. Stern, *Astrophys. J. Lett.* **734**, L5 (2011).
[12] W. B. Latter, C. K. Walker, and P. R. Maloney, *Astrophys. J. Lett.* **419**, L97 (1993).
[13] <http://ned.ipac.caltech.edu/level5/Sept07/Omont/Omont2.html#2.4>.
[14] C. Tian and C. R. Vidal, *J. Phys. B* **31**, 895 (1998).
[15] C. Tian and C. R. Vidal, *Phys. Rev. A* **59**, 1955 (1999).
[16] M. A. Mangan, B. G. Lindsay, and R. F. Stebbing, *J. Phys. B* **33**, 895 (2000).
[17] O. J. Orient and S. K. Srivastava, *J. Phys. B* **20**, 3923 (1987).
[18] J. M. Curtis and R. K. Boyd, *J. Chem. Phys.* **80**, 1150 (1984).
[19] P. Lablanquie *et al.*, *Phys. Rev. A* **40**, 5673 (1989).
[20] M. Lundqvist, P. Baltzer, D. Edvardsson, L. Karlsson, and B. Wannberg, *Phys. Rev. Lett.* **75**, 1058 (1995).
[21] H. Ren, R. Ma, J. Chen, X. Li, H. Yang, and Q. Gong, *J. Phys. B* **36**, 2179 (2003).
[22] C. Cornaggia, J. Lavancier, D. Normand, J. Morellec, P. Agostini, J. P. Chambaret, and A. Antonetti, *Phys. Rev. A* **44**, 4499 (1991).
[23] L. Adoui, C. Caraby, A. Cassimi, D. Lelièvre, J. P. Grandin, and A. Dubois, *J. Phys. B* **32**, 631 (1999).
[24] I. Ben-Itzhak, S. G. Ginther, V. Krishnamurthi, and K. D. Carnes, *Phys. Rev. A* **51**, 391 (1995).
[25] H. O. Folkerts, F. W. Blik, M. C. de Jong, R. Hoekstra, and R. Morge, *J. Phys. B* **30**, 5833 (1997).
[26] G. Sampoll, R. L. Watson, O. Heber, V. Horvat, K. Wohrer, and M. Chabot, *Phys. Rev. A* **45**, 2903 (1992).
[27] M. Tarisien *et al.*, *J. Phys. B* **33**, L11 (2000).
[28] R. D. Dubois, T. Schlatholter, O. Hadjar, R. Hokestra, R. Morgenstern, C. M. Doudna, R. Feeler, and R. E. Olson, *Europhys. Lett.* **49**, 41 (2000).
[29] V. Krishnamurthi, K. Nagesha, V. R. Marathe, and D. Mathur, *Phys. Rev. A* **44**, 5460 (1991).
[30] T. Masuoka, *J. Chem. Phys.* **101**, 322 (1994).
[31] G. Dawber, A. G. McConkey, L. Avaldi, M. A. MacDonald, G. C. King, and R. I. Hall, *J. Phys. B* **27**, 2191 (1994).
[32] D. Mathur, E. Krishnakumar, K. Nagesha, V. R. Marathe, V. Krishnamurthi, F. A. Rajgara, and U. T. Raheja, *J. Phys. B* **26**, L141 (1993).
[33] R. Singh, P. Bhatt, N. Yadav, and R. Shanker, *Meas. Sci. Technol.* **22**, 055901 (2011).
[34] P. Bhatt, R. Singh, N. Yadav, and R. Shanker, *Phys. Rev. A* **84**, 042701 (2011).
[35] P. Bhatt, R. Singh, N. Yadav, and R. Shanker, *Phys. Rev. A* **82**, 044702 (2010).
[36] P. Bhatt, R. Singh, N. Yadav, and R. Shanker, *Phys. Rev. A* **85**, 042707 (2012).
[37] J. H. D. Eland, *Mol. Phys.* **61**, 725 (1987).
[38] P. Bhatt, R. Singh, N. Yadav, and R. Shanker, *Phys. Rev. A* **85**, 034702 (2012).
[39] L. H. Andersen, J. H. Posthumus, O. Vahtras, H. Ågren, N. Elander, A. Nunez, A. Scrinzi, M. Natiello, and M. Larsson, *Phys. Rev. Lett.* **71**, 1812 (1993).
[40] R. Püttner *et al.*, *Chem. Phys. Lett.* **445**, 6 (2007).
[41] S. W. J. Scully, J. A. Wyer, V. Senthil, and M. B. Shah, *J. Electron Spectrosc. Relat. Phenom.* **155**, 81 (2007).
[42] G. Handke, F. Tarantelli, and L. S. Cederbaum, *Phys. Rev. Lett.* **76**, 896 (1996).
[43] P. Kumar and N. Sathyamurthy, *Pramana J. Phys.* **74**, 49 (2010).